Accepted Manuscript

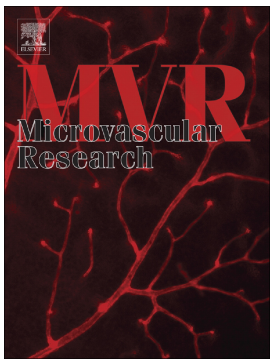

The pivotal role of angiogenesis in a multi-scale modeling of tumor growth exhibiting the avascular and vascular phases

Hooman Salavati, M. Soltani, Saeid Amanpour

PII: S0026-2862(17)30255-8
DOI: doi:10.1016/j.mvr.2018.05.001
Reference: YMVRE 3791

To appear in: *Microvascular Research*

Received date: 25 November 2017
Revised date: 28 April 2018
Accepted date: 3 May 2018

Please cite this article as: Hooman Salavati, M. Soltani, Saeid Amanpour , The pivotal role of angiogenesis in a multi-scale modeling of tumor growth exhibiting the avascular and vascular phases. The address for the corresponding author was captured as affiliation for all authors. Please check if appropriate. Ymvre(2017), doi:10.1016/j.mvr.2018.05.001

The Pivotal Role of Angiogenesis in a Multi-scale Modeling of Tumor Growth Exhibiting the Avascular and Vascular Phases

Hooman Salavati[1], M. Soltani[2,3,4,5,6], Saeid Amanpour[6]

[1] Department of Mechanical Engineering, Pardis Branch, Islamic Azad University, Pardis, Iran.

[2] Department of Mechanical Engineering, K. N. Toosi University of Technology, Tehran, Iran.

[3] Computational Medicine Center, Tehran, Iran.

[4] Division of Nuclear Medicine, Department of Radiology and Radiological Science, School of Medicine, Johns Hopkins University, MD, USA.

[5] Department of Earth & Environmental Sciences, University of Waterloo, Ontario, Canada

[6] Cancer Biology Research Centre, Cancer Institute of Iran, Tehran University of Medical Sciences, Tehran, Iran.

Abstract

The mechanisms involved in tumor growth mainly occur at the microenvironment, where the interactions between the intracellular, intercellular and extracellular scales mediate the dynamics of tumor. In this work, we present a multi-scale model of solid tumor dynamics to simulate the avascular and vascular growth as well as tumor-induced angiogenesis. The extracellular and intercellular scales are modeled using partial differential equations and cellular Potts model, respectively. Also, few biochemical and biophysical rules control the dynamics of intracellular level. On the other hand, the growth of melanoma tumors is modeled in an animal in-vivo study to evaluate the simulation. The simulation shows that the model successfully reproduces a completed image of processes involved in tumor growth such as avascular and vascular growth as well as angiogenesis. The model incorporates the phenotypes of cancerous cells including proliferating, quiescent and necrotic cells, as well as endothelial cells during angiogenesis. The results clearly demonstrate the pivotal effect of angiogenesis on the progression of cancerous cells. Also, the model exhibits important events in tumor-induced angiogenesis like anastomosis. Moreover, the computational trend of tumor growth closely follows the observations in the experimental study.

Keywords: Tumor Growth, Tumor-induced Angiogenesis, Multiscale Modeling, Cellular Potts Model, Animal Modeling

Introduction

Nowadays cancer is one of the major threats to human life. Relying on this importance, many researches have studied the various aspects of tumors biology in order to obtain an understanding of the related mechanisms, and to predict optimal anti-cancer treatments. Procedurally, appearance and progression of solid tumors are the main dynamics of most cancers [1]. Accordingly during the last few decades, the mechanisms of solid tumor growth attract the attention of many cancer-related researchers [2]. Solid tumor is an unusual cell population appearing due to the lack of normal regulation on cells growth mechanisms, which consequently initiates excessive cells proliferation. During the first phase of tumor development, entitled avascular growth, due to the limitation of oxygen diffusion into living tissues, the concentration of oxygen is decreased around the tumor core cells. Consequently, the internal machine of each hypoxic, oxygen-deprived, cell switches the phenotype of the cell step by step from proliferating to quiescent, and finally to necrotic. In this situation, necrotic cells secrete a variety of pro-angiogenic factors into the surrounding tissue [3], such as diverse types of growth factors, different types of regulator proteins like vascular endothelial growth factor (VEGF) [4]. However, these tumor angiogenic factors (TAFs) stimulate the microenvironment, particularly endothelial cells (ECs), and make it undergoing into the vascular phases of evolution [5]. All in all, vascular networks start to grow toward avascular tumor rely on complex amounts of signaling pathways [6] and a process so called tumor-related angiogenesis is begun [7]. Angiogenesis acts as a switch to reactivate quiescent cells and turns tumor growth phase from avascular to vascular. Generally, it has been demonstrated that tumor size in avascular phase is limited to a diameter of 1 to 2 millimeter and tumor cell population is limited [8], however, the tumor growth in absence of mechanical barriers or therapies is extremely progressive during the

vascular stage. Moreover, the tumor invasion and metastasis are more likely to happen in vascular stage.

Mechanisms involved in tumor growth engages complex multicellular dynamics in different spatio-temporal scales including intracellular, intercellular and extracellular scales [9]. Despite the helpful understandings of tumor growth processes obtained by experiments tied up with recent imaging modalities [10, 11], it is hard to evaluate all the various multi-scale phenomena occurring during tumor growth in experimental studies. In this context, a multi-scale modeling embedding various spatio-temporal scales involving in tumor growth would make an acceptable sight of such intricate procedure.

Mathematical Modeling of Tumor Growth

Mathematical and computational approaches facilitate several strategies to rebuild the multi-scale processes involved in tumor growth. Over the last two decades a number of computational models have been developed to investigate the nature of tumor growth. In several studies, continuous models act like a black box hiring a series of advection-diffusion-reaction equations to describe tumor dynamics in the border [12]. These models do not provide details on many important processes such as cellular interactions. On the other hand, discrete approaches consider the tumor as a population of interacting cells or agents [13] which have the ability to model important cellular functions like migration [14]. Accordingly, the discrete models, such as cellular automata (CA) approaches [15], obtain more naturalistic presentation of the process, which is more biologically desired too. However, the drawback of discrete modeling is the high computational cost. In the third approach, hybrid models exploit a combination of continuous and discrete models considering the optimized approach for each scale [16]. Also, it has been demonstrated that the integration of various spatio-temporal processes in a hybrid model usually

provides a solid context to simulate diverse multi-scale biological phenomena such as tumor growth.

Hybrid models of solid tumor growth have been involved into three categories including avascular growth, tumor-related angiogenesis, and vascular growth. While the vascular growth is known as the hallmark of cancer progression [17], the majority of previous models, involving most of the multi-scale models, have solely studied the avascular growth [18]. In the most similar work to the current study regarding the modeling approach, Jiang et al. provided a hybrid frame work to monitor tumor growth during avascular stage [19]. Alemani et al. combined cellular automata (CA) with lattice Boltzmann method to model avascular tumor growth along with the immune system responses [20]. Also, Dormann and Deutsch modeled the tumor growth using the CA to simulate the growth of a self-organized avascular tumor [21], and recently Ghadiri and coworkers developed a multi-scale model of tumor growth based on an agent-based framework [22]. A comprehensive account of the mathematical models of avascular tumor growth and relevant literature is found in the works of Roose et al [23] and, Cristini and Lowengrub [24]. All in all, despite the mathematical and computational advances in the tumor growth modeling, these models due to lack of at least vascular phase simulation are inadequate. Hopefully in the recent years, the development of hybrid models offer a path toward the comprehensive as well as predictive modeling of tumor growth [25]. In the one of the most cited works on the vascular tumor modeling, Macklin and coworkers coupled a model of tumor growth with a model of tumor-induced angiogenesis to study the vascular remodeling [26]. Shirinifard et al presented a multi-cell simulation of a generic simplification of vascular tumor growth [27]. Lesart and coworkers combined a computational model with a mouse model to investigate the effects of vascular network during tumor development [28]. Tang et al. simulated

the tumor growth affected by angiogenesis using a system of partial differential equations [29]. Also, Xu et al using phase fields and a reaction diffusion equation simulated the tumor growth coupled with angiogenesis [30]. The articles of Oden et al. [25] along with Ng and Frieboes [18] study provide a full background on multi-scale modeling of vascular tumor.

Although the achievements of previous works would be considered as a big step for the development of a multi-scale in-silico model of tumor growth, previous models hardly hold to be a comprehensive one because of at least one of the following reasons. Firstly, they often have not gathered together the three major phases of tumor growth including avascular growth, angiogenesis and vascular growth. Moreover, the majority of previous studies have been used prescribed rules in the all aspects of modeling which eliminate the originality of the results. In the current study, we present a comprehensive multi-scale model of solid tumor growth that simulates avascular and vascular tumor growth as well as tumor-induced angiogenesis using no prescribed rules except elementary dynamics in the intracellular environment. We developed a hybrid model which a cell-based model, cellular Potts model (CPM), describes the cellular dynamics in the microenvironment, and two partial differential equations (PDEs) evolve oxygen and TAF diffusion in the domain.

Materials and methods

Animal Experiments

All the experimental procedures, including what has related to the development, sampling and testing murine cancer models were taken place in the animal lab of Cancer Biology Research Center (CBRC) of Tehran University of Medical Sciences (TUMS) that is placed in Imam

Khomeyni Hospital Complex. Indeed, CBRC obtained the TUMS Cancer Research Center's (CRC) approval for all protocols were followed in this article in the way of ethical code.

Tumor model

Three Male C57Bl/6 mice, 12 weeks of age and approximately 20 up to 26 gr of weights, were purchased from Advanced BioModel Co/ P. B16/F10 (CRL-6475) Melanoma cells line were obtained from Pasture Institute of Iran. Cells were cultured in DMEM + 10% FBS + 2mML-Glutamine with the concentration of 1×10^6 cells/100 µl and 20 ul of the cultured media were injected subcutaneously. This way, mice were anaesthetized by peritoneum injection of ketamine 80-100 mg/kg and xylazine 10-12.5 mg/kg. After 15 days, palpable tumors were touched under mice skins. Mice were sacrificed in the day 15 using cervical dislocation method. The tumors were excised and sliced into small pieces. Syngeneic transplantations were conducted using three other C57Bl/6 using these slices. For the sake of the transplantation, mice were chosen from similar strains and anaesthetized in similar protocol depicted above. Sliced tumors were transplanted intracutaneously using a pair of forceps. The mice tumor's evolutions were analyzed every three days for the period of one month using digital caliper every 3 days after transplantation and the table 1 shows the results.

Table 1. Tumor sizes measurement in the period of 30 days for 3 mice of control.

	MOUSE 1 (mm^3)	**MOUSE 2 (mm^3)**	**MOUSE 3 (mm^3)**	**AVERAGE**
DAYS 3	44.1	28.2	49.7	40.7
DAYS 6	116.1	25.9	152.8	98.3
DAYS 9	45.6	218.9	242.5	169
DAYS 12	16.9	50.3	88.9	52

DAYS 15	153.2	1045.3	708.6	635.7
DAYS 18	120.6	1077.4	2098.5	1098.8
DAYS 21	567.5	1951.1	6495.1	3004.6
DAYS 24	711	3972.5	9805.3	4829.6
DAYS 27	1599.3	6176.4	12902	6892.6
DAYS 30	2923.5	11760.9	16651.2	10445.2

Multi-Scale Modeling of Tumor Growth

Our multi-scaled model couples angiogenesis and tumor growth and it evolves the processes in three levels which are the extracellular, intercellular and intracellular levels. Accordingly, at the extracellular level, nutrients diffuse from the nearby parent vessels, and make a gradient in the tumor surrounding tissue. Also, during angiogenesis phase, the hypoxic cells in the center of fast proliferative tumor cells mass secrete the TAF into extracellular environment. Consequently, at the intracellular level, the mechanical and chemical signals actuate the internal machine of each cell, including cancerous cells and tumoral endothelial cells, to change the cells' phenotype. Finally, at the intercellular level, cells activation including cancerous cells proliferation and, ECs proliferation and migration occurs.

At the extracellular level a diffusion-reaction equation controls oxygen diffusion into nearby tissue and also, it calculates oxygen consumption of cancerous cells [16]. Moreover, the concentration of TAF is calculated by a diffusion equation. At the cellular level, tumor is treated as a mass of agents. Also, the process of sprouting angiogenesis depends on endothelial cells dynamics. Accordingly, the cellular Potts models (CPM) is employed to reproduce cellular interactions in the model. CPM is a cell-based model working according to energy minimization

principle that was developed by Glazier and Graner [31]. In CPM, based on the Hamiltonian which is corresponded to total energy in the system, Hamiltonian terms describe the cellular dynamics in the model. Accordingly, each lattice total energy is calculated in each time step to decide what change in the lattice configuration is acceptable. Mainly, Intercellular interactions occur only at the cell's surface. Therefore, the main machine of CPM are the surface fluctuations of cells controlling by the Hamiltonian [32].

Model Domain and Geometry

The computational domain is a cube with a side of 15 mm, which at the onset of simulation thousand tumor cells are located at the center of domain, ready to grow in respect to available amount of oxygen. Also, during the initiation of vascular phase, the angiogenic sprout would grow form the parent vessel locating on the domain sides. The avascular tumor in the earliest phase of growth consists of proliferating cells. As tumor grows, due to oxygen deficiency in the center of tumor, hypoxic cells have to change their phenotype from proliferating to quiescent. However, peripheral tumor cells still proliferating and tumor growth is not halted at this stage. After a while, the quiescent cells die, and necrotic core is generated. Subsequently, hypoxic cells release angiogenic factors to stimulate nearby vessels to actuate sprouting angiogenesis. Consequently, after sprouts maturation, the growth of new formed vasculature increases the amount of oxygen and nutrients around hypoxic region. After reaching a threshold for triggering cellular growth, quiescent cells are activated, and starts to growth exponentially. Fig. 1 illustrates a schematic design of the computational domain.

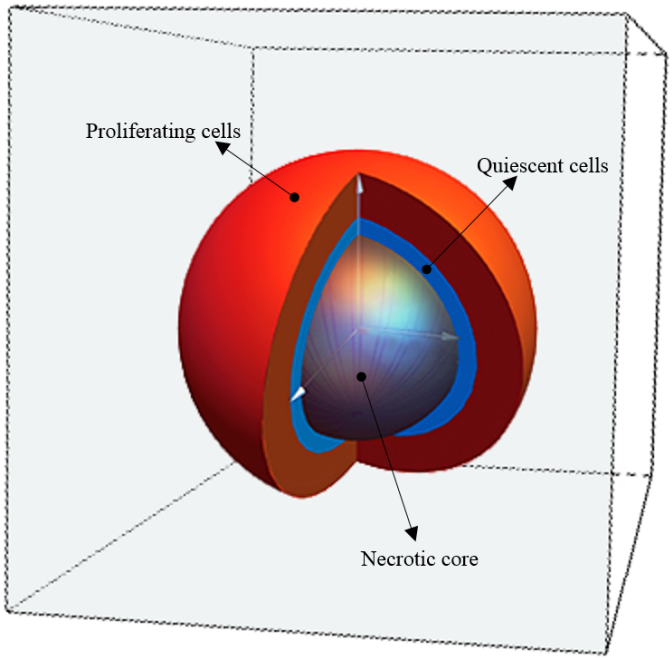

Figure 1: Model domain and its component. Necrotic core (gray), quiescent cells (blue) and proliferating cells (red) are located in the tumor matrix.

Extracellular Level

Cancerous cells are in a tight interaction with surrounding microenvironment. The microenvironment dynamics is controlled by the amount of certain biochemical substances. During tumor growth, the main regulatory substances are TAF as well as oxygen and glucose which in the literature is denoted by nutrients. In the current model, the available amount of oxygen for each cell in the surrounding decides the cancerous cells phenotype. Mathematically, a diffusion-reaction equation is able to describe the diffusion of oxygen in the domain as follows [17].

$$\frac{\partial V}{\partial t} = D_{O_2} \nabla^2 V + C(x, y, z) \qquad (1)$$

In equation (1), V (x, y, z, t) is the concentration of oxygen in domain. D_{O_2} is the oxygen diffusion constant which it has a positive and homogenous value all over the domain. C is the consumption rate of oxygen by cancerous cells, which varies depending on the tumor cells phenotypes. The C defines as following [17]

$$C = C_0 \frac{V - V^T}{V^O - V^T} \tag{2}$$

In equation 2, C_0, V^O and V^T respectively are initial oxygen consumption rate, oxygen optimize concentration and oxygen threshold concentration [17].

In this level, oxygen diffuses though extracellular matrix (ECM), which in the current modeling, the ECM was modeled implicitly. Also, the diffusion constant has same value all over the domain including. Considering these simplifications, the boundary conditions on the tumor will be [17];

$$V = V^O \tag{3}$$

During angiogenesis, TAF is secreted into the ECM by tumor hypoxic cells. The TAF has constant decay rate and it uptakes by ECs [9]. The below diffusion equation describes the TAF dynamics in the domain:

$$\frac{\partial V}{\partial t} = D_{TAF} \nabla^2 V - \lambda V - B(x, y, V) \tag{4}$$

where V (x, y, t) denotes the TAF concentration and D_{TAF}, λ, and B are the TAF diffusion coefficient, TAF decay rate, and TAF uptake function, respectively. The coefficient of diffusivity for TAF in tissue, $D_{TAF} > 0$, is assumed to be constant all over the simulation domain. The rate of

TAF decay, $\lambda > 0$, is also assumed to be constant, and B (x, y, V) is a function that defines the amount of TAF uptake by each EC [9]. The uptake function is [9];

$$B(x, y, V) = \begin{cases} (x, y) \in EndothelialCell, & \begin{cases} \beta & if\ \beta \le V \\ V & if\ \beta > V \end{cases} \\ (x, y) \notin EndothelialCell, & 0 \end{cases} \quad (5)$$

In Eq. 5, β is the maximum amount of TAF which can be bound to an EC's receptors. At first there is no amount of TAF till the cancerous cells become hypoxic. Procedurally, the TAF source reaches a constant concentration denoted with *S* [9].

At the onset of simulation, it is assumed that oxygen concentration is constant at the domain. At avascular phase, growing cells consume available oxygen and hence, the concentration of oxygen decreases around the tumor. Consequently, the released TAF actuate the angiogenesis process, and a new vascular network forms around tumor. Accordingly, at this vascular stage, growing vasculatures bring new supply of oxygen which help quiescent cells to survive and, proliferate.

Cellular Level

Cells are the main machine in cellular level of cellular Potts model (CPM). In this level the main approach for capturing cellular dynamics is to set an energy, based on Hamiltonian, for each distinct physiological phenomena occurring at the cell-cell interaction.

In the CPM lattice, matrix, necrotic core and quiescent cells IDs are 0, 1 and 2 respectively. Also, each proliferating cell has unique ID number starting from 3. Moreover, during angiogenesis, each EC is identified in the model with a specific ID. Fig. 2 shows a typical configuration of CPM lattice.

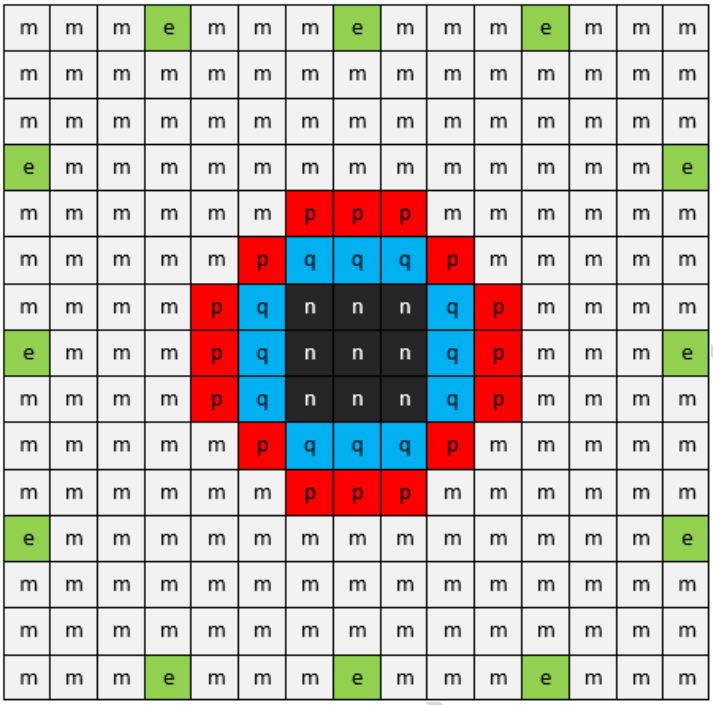

Figure 2: Typical 2D configuration of the domain lattice in CPM. *The light gray (m), green (e), red (p), blue (q) and dark gray (n) pixels are tumor surroundings matrix, proliferating, quiescent and necrotic cells, respectively.*

The main biological phenomena controlling the cellular environment during tumor growth are cells adhesion, growth and migration. Cell adhesion is a key biological characteristic for preserving multicellular structures. Cellular adhesion is core of many morphogenetic processes regulating mechanical interactions between cells. For instance, cell migration and cell sorting are samples of important morphogenetic processes controlling by the cellular adhesion molecules [33]. The adhesion energy comes from hydrogen and ionic bonds that keep cells and their adhesion cooperative together [9]. The mechanical role of adhesion is to provide the requisite energy needed for the cohesive attachment of cells to their surroundings, this energy can be described as following

$$E_{adhesion} = \sum_{domain} J_{\tau,\tau'}(1-\delta_{\sigma,\sigma'}) \qquad (6)$$

J is the adhesion energy between two entities τ and τ'. σ and σ' are numbers of two adjacent lattice sites and δ is the Kronecker delta. Kronecker delta has nonzero value only in lattice sites with different cells type in the neighborhood.

Generally in absence of any treatment and physical barrier, Cancerous and endothelial cells grow until reach the maximum size called target volume. After reaching the target volume, the cells will be entering into mitosis cycle and each mature cell is divided into two separate cells. The next energy term provide cell growth and cell deformation required energy [19]:

$$E_{volume} = \sum_{cells} \gamma_{\tau}(a_{\sigma} - A_{\sigma}^{T})^{2} \quad (7)$$

In equation (5) a_{σ} is the current volume of cell and A_{σ}^{T} is the target volume of the each cell. γ_{τ} is the resistance of cells to the volume change that is interpreted as cells elasticity. We assume that without any other external forces and ample nutrition, the cancerous cells would grow until getting double of its initial volume, which sets as the target volume. As far as cell volume is less than the target volume, every change in the cell that increases its volume, reduces the total energy of the system and helps to accept the change in the lattice configuration.

To keep pixels continuity in a unique cell, another Hamiltonian term is considered in the total energy to avoid cell rupturing during migration and proliferation. Accordingly, if the summation of pixels' volume for each cell (a_{σ}) would not equal the summation of continuous pixels' volume of that cell ($a_{\sigma'}$), the total energy increased drastically by the following term and prevent any change in system [9]:

$$E_{continuity} = \sum_{cells} \alpha(1 - \delta_{a_{\sigma}, a_{\sigma'}}) \quad (8)$$

In the above equation α is continuity constant which its value is noticeably high.

In the model, cancerous cells interactions could be modeled through Hamiltonian by combination of adhesion, growth and continuity energies.

$$E_{TumorGrowth} = E_{adhesion} + E_{volume} + E_{continuity} \tag{9}$$

At the onset of vascular stage, endothelial cells of nearby vessels are induced by TAF to migrate toward the tumor by chemotaxsis strategy. Chemotaxis mainly is determined by the TAF gradient in the domain. Therefore, a simple relation between chemotaxis and TAF gradient could indicate its contribution to total energy. Haptotaxis is the directed movement of cells controlled by the relative connection due to peripheral cells adhesions. Since the different adhesion energies are considered between entities, the model inherently contains haptotaxis energies [9]. Due to chemotactic migration, ECs move in the direction of increasing TAF concentration. Phenomenologically, chemotaxis speed has a proportion to the TAF gradient. Consequently, chemotactic force is proportional to the chemical gradient [34], and it is possible to construct a proper chemotaxis energy, that is proportional to the local chemical gradient as follows,

$$E_{chemotaxis} = \sum_{domain} \chi_\sigma \Delta V \tag{10}$$

where χ_σ is the effective chemical potential of ECs and ΔV is the TAF gradient. The response of ECs and Tip cells to chemotaxis stimuli is different. Thus, different effective chemical potentials are considered for ECs and Tip cells in the model.

Considering the nature of angiogenesis process, the interaction between ECs and tumor can be described as below

$$E_{Angiogenesis} = E_{adhesion} + E_{volume} + E_{chemotaxis} + E_{continuity} \quad (11)$$

Every changes in the lattice configuration is based on a simple rule that ensures system randomness. Procedurally, a lattice site, (i, j), is selected at random, and one of the unlike nearest neighbors, (i', j'), is selected randomly. The total energy of the system is computed before and after any proposed update in lattice. If the total system energy is reduced due to the change, it is accepted [35]; otherwise, the update is accepted with a Boltzmann probability [9]

$$P_{acceptance} = \exp\left(\frac{-\Delta E_{total}}{kT}\right) \qquad \Delta E > 0 \quad (12)$$

Where *k* is the Boltzmann constant and T is a measure of system disorder or cell membrane fluctuations.

Intercellular Level

In this scale, the model considers few rules between extracellular and intercellular levels for the following cellular behaviors. For cancerous cells, oxygen vital threshold along with the competition between cells for acquiring space to grow determine the phenotype of each cell [19,36]. Accordingly, in the model, if a tumor cell does not grow in a time equal to the average time for a tumor cell to grow one pixel, the cells phenotype changes to quiescent, and cellular growth is stopped. Afterwards, if the oxygen concentration gets below a vital threshold, denoted with t_v, quiescent cells die via necrosis, and angiogenic signaling is initiated by necrotic cells [37].

Model Parameters

In current model, the physiologic and physical properties for various cells type are different including cell cycle stage, metabolism rate, cellular adhesion and cells target volume. As

surrounding matrix pixels has no target volume, peripheral cancerous cells can easily evade and growth in this environment. Also, target volume of necrotic cells is equal to the last volume of cells before necrosis.

A list of all parameter values used in our model provided in Table 2. Generally, the parameter values involved in the reaction-diffusion equation obtained from empirical data sets [38-44]. Since there is no available experimental value for the parameters involved in the cell-based model, they were manually tuned to emulate observed phenomenological behaviors, and to follow the experimental results. However, the range of parameters tuning adopted from the experiments, and basic biological knowledge [19]. Accordingly, cellular bounds indicates that the binding between two ECs or two cancerous cells is much stronger than binding of any other constituent types in the EC-ECM or tumor cell-ECM interactions [9, 19]. Also, regarding the binding of tumor cells, due to low impact of cellular adhesion in the model comparing to growth and proliferation affinities, there would no significant impact by choosing other values [19]. The values of membrane elasticity is defined somehow to reflect the natural deformation of each cell during growth. For instance, the elasticity constant of necrotic cells is assumed relatively high in order to express necrotic core as a solid body.

Table 2. Values of model's constants

Parameter	Symbol	Dimensions	Model Value
Length Scales	$L_{1,2,3}$	L	3000μm
Oxygen Diffusion	D_{O2}	L^2/T	1.65×10^3 $\mu m^2/s$ [38,39]
Initial Consumption of Proliferating Cells	$C_{0\text{-}P}$	$M/T/L^3$	8.97×10^{-9} pg/s/voxel [40]
Initial Consumption of Quiescent Cells	$C_{0\text{-}Q}$	$M/T/L^3$	4.15×10^{-9} pg/s/voxel [40]
Initial Consumption of Necrotic Cells	$C_{0\text{-}N}$	$M/T/L^3$	0.00 pg/s/voxel
Vital Threshold	t_V	M	4.48×10^{-3} pg/voxel [41]
TAF Diffusion	D_{TAF}	L^2/T	0.1 $\mu m^2/s$ [42]
TAF Decay	λ	T^{-1}	1.8×10^{-4} s^{-1} [42]
TAF uptake	β	M/cell/T	1.66×10^{-5} pg/EC/s [43]
TAF Source	S	M/L	0.035 pg/voxel [44]
Activation Threshold	ν_a	M	0.0001 pg [7]
Proliferating-Matrix Adhesion	J_{pm}	E/L	16 [19]
Quiescent-Matrix Adhesion	J_{qm}	E/L	14 [19]
Necrotic-Matrix Adhesion	J_{nm}	E/L	12 [19]
Proliferating-Proliferating Adhesion	J_{pp}	E/L	28 [19]
Proliferating- Quiescent Adhesion	J_{pq}	E/L	28 [19]
Proliferating-Necrotic Adhesion	J_{pq}	E/L	24 [19]
Quiescent- Quiescent Adhesion	J_{pn}	E/L	28 [19]
Necrotic-Necrotic Adhesion	J_{qq}	E/L	24 [19]
Quiescent-Necrotic Adhesion	J_{nn}	E/L	22 [19]

EC-EC Adhesion	J_{qn}	E/L	30 [46]
EC-Matrix Adhesion	J_{ee}	E/L	66 [47]
Matrix-Matrix Adhesion	J_{em}	E/L	85 [46]
Proliferating Cells Elasticity	γ_p	E/L^4	2
Quiescent Cells Elasticity	γ_q	E/L^4	8
EC Membrane Elasticity	γ_e	E/L^4	0.8 [45]
Chemotactic Sensitivity	χ	E/conc.	1.1×10^6 [45]
Boltzmann Temperature	kT	E	2.5 [9]

The sensitivity analysis of parameters is conducted by changing one parameter value fixing other parameters involved in the modeling. Accordingly, the results show by choosing relatively smaller values for adhesion energies ($J_{\tau,\tau'}$) than the reported values in Table 2, generally the cells bonds become stronger. However, it unrealistically simulates the cells shapes, elongation and especially sprouts morphology. On the other hand, greater values of adhesion energies decrease the cellular contacts disintegrating the cells adhesive connections. Particularly doubling the adhesion value for endothelial cells, J_{ee} = 60, splits up the endothelial cells during sprouting. Moreover, it fades the migration cues of endothelial cells during haptotactic migration. Regarding the elasticity constants (γ_τ), any smaller value than the current measure accelerates the growth speed of all type of cells and subsequently it increases the size of tumor. However, this forces the cells to deviate the target volume, which is not biologically acceptable. Greater amount of elasticity also makes cellular growth harder which reduces the growth rate, and increases the time of computation. Regarding the effect of chemotactic sensitivity value on the model, a smaller value like $\chi = 1\times10^4$ decreases the chemotaxis potency during ECs migration and

fails the sprouting angiogenesis. Otherwise, a larger value of chemotactic sensitivity endangers the ECs continuity during migration. The value of *kT* affects the membrane fluctuations of cells in the model. Accordingly, the higher values increase the membrane fluctuations, and smaller values decrease the membrane fluctuations in the simulation.

Results and Discussion

The simulation initiates with a tumor consists of thousand cancerous cells. Also, at the beginning of angiogenesis, 36 single endothelial from four parent vessels cells appears at the border of the domain receiving the signal from TAF stimulation, and they are lined up for migration toward tumor. In another word, after uptaking the TAF by ECs, they start to grow, proliferate and migrate toward the hypoxic cells. The results are presented in two major parts. Firstly, the evolution of tumor in avascular phase, in the absence of adequate nutrients, is presented. Subsequently, the results of avascular growth are evaluated by the experimental results adopted from Jiang et al work [17]. In the next part, the simulations of tumor growth promoted by the angiogenesis process is demonstrated. Fig. 3 shows the earliest growth of avascular tumor in the first four days. Results in Fig. 3 illustrate that this cluster of tumor cells feeding from the available nutrients in the surrounding grows up to ten times in just first four days.

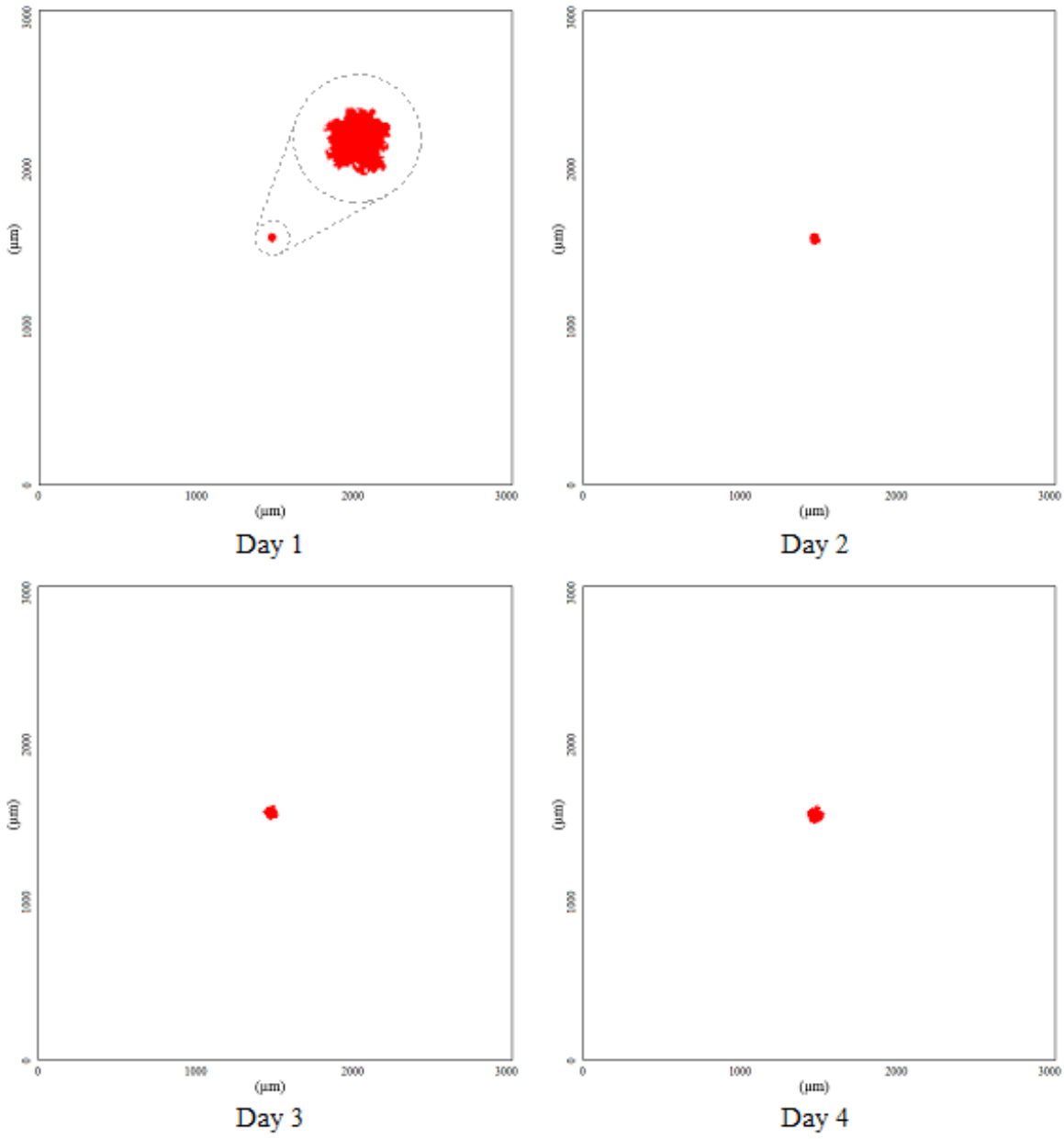

Figure 3: The avascular tumor is growing ten times in the first four days of modeling. The simulation starts with a cluster consists of thousand proliferating cancerous cells (the red cluster) located at the center of domain.

Fig. 4 illustrated the formation of quiescent cells in the inner part of tumor spheroid .After a while, peripheral cells in the tumor spheroid consume oxygen in the environment, and decrease the oxygen diffusion to central parts of tumor. Moreover, the physical challenges between peripheral and inner cells for growth prevent inner core tumor cells from growing. As a result of

these conditions, the substantial part of inner cells changes their phenotype to quiescent. In Fig. 4, it is possible to observe that the interface between quiescent and proliferating cells moves continuously toward tumor surface. Also, even though the gradient of tumor growth is slower in this situation, however, tumor pursue its growth up to four times.

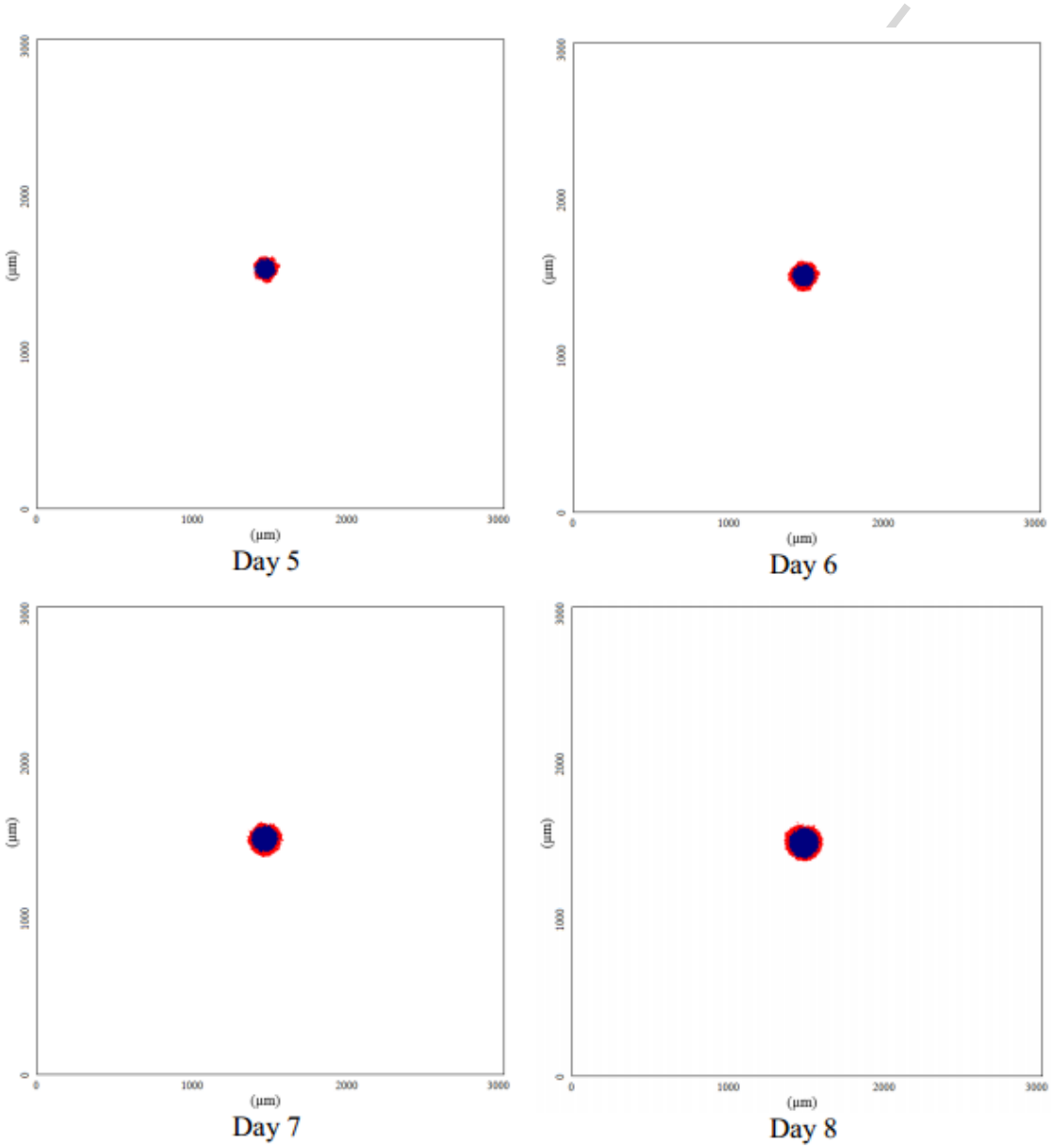

Figure 4: Multiple scenes of tumor growth in second four days. Central cells due to oxygen shortage turn from proliferating (red) to quiescent (blue) cells.

After cell quiescence, due to severe oxygen shortage in the tumor core cells, necrosis is occurred. Considering this theory, in the model necrosis occurs when the oxygen concentration does not satisfy oxygen vital threshold (t_v). In Fig. 5, the third four days of tumor growth is shown, which the necrosis occurs in day 10. Results show that by forming the necrotic core in avascular phase, tumor does not grow more than five percent per day.

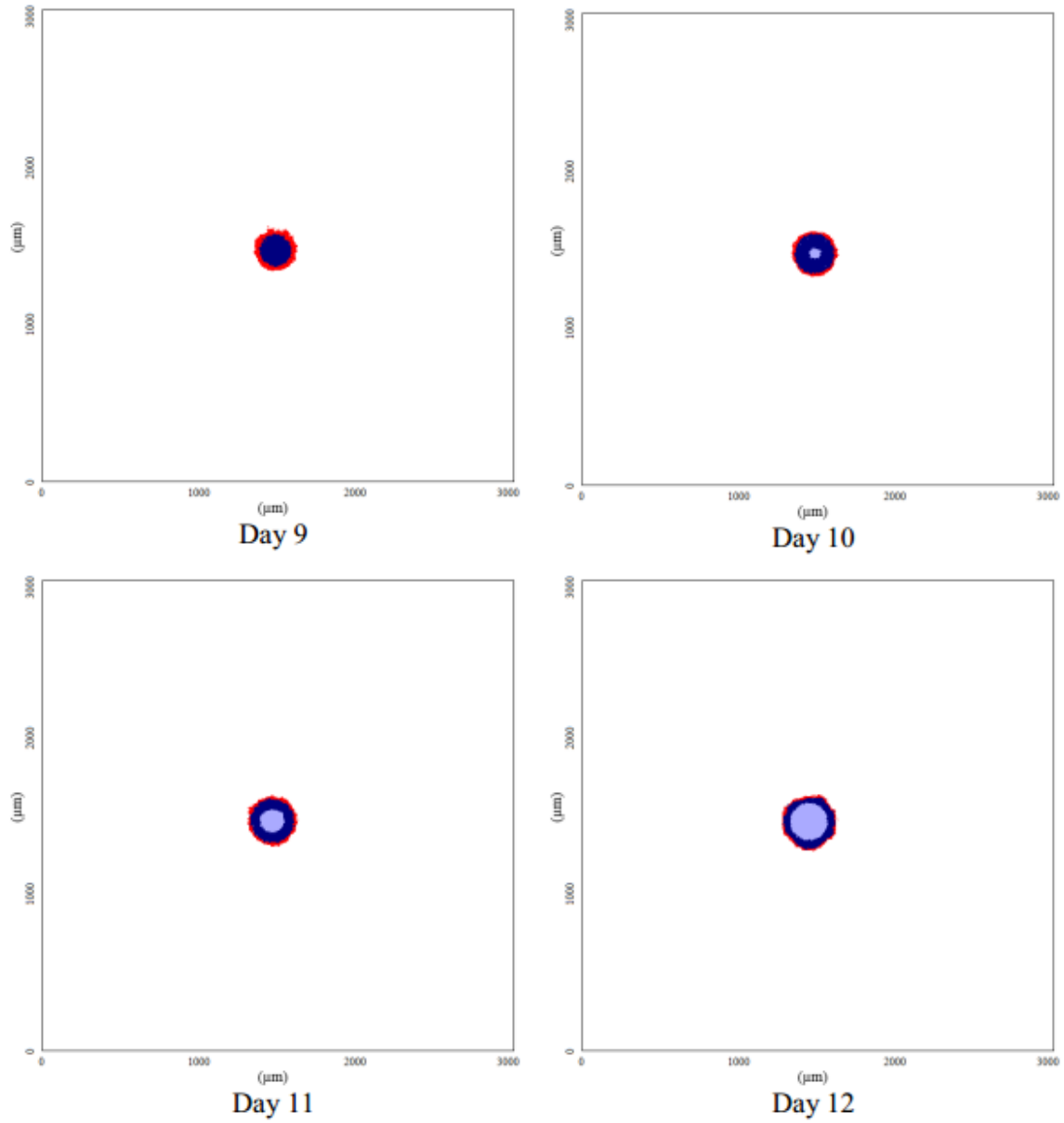

Figure 5: Multiple scenes of tumor growth in third four days. Along with oxygen shortage consistency, quiescent cells (blue) die and necrotic core (gray) is formed.

It is possible to evaluate the trend of tumor growth produced by the model with an experiment conducted by Jiang et al [17] in Fig. 6. The comparison demonstrates that the computational results, considering the model simplifications, nearly follows the experimental observation.

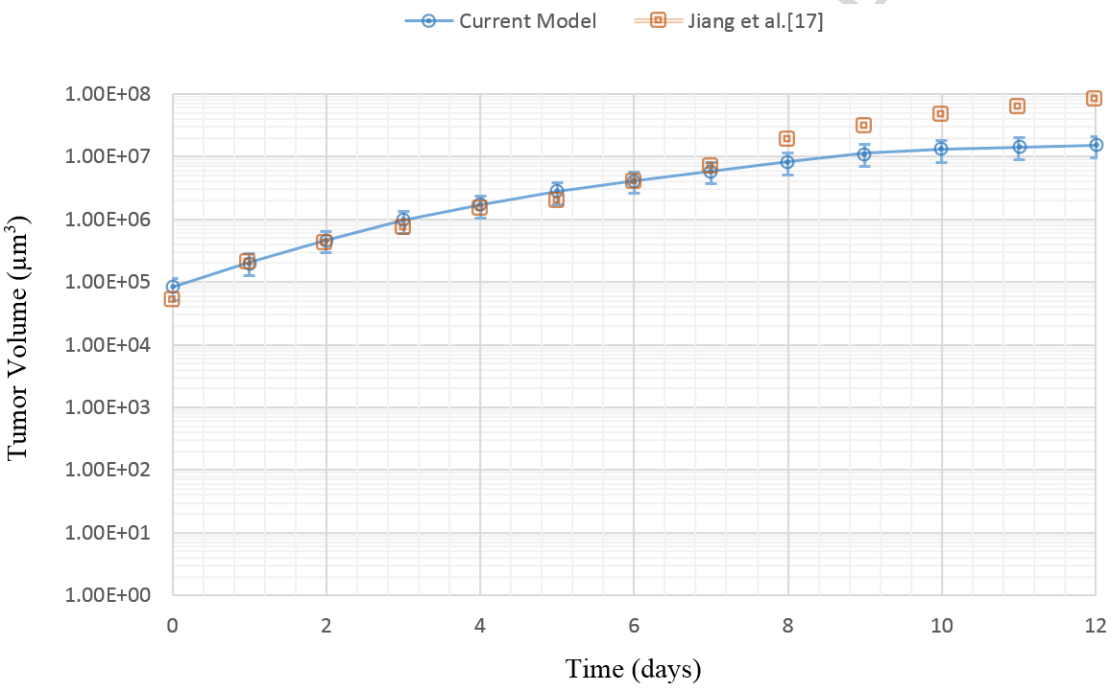

Figure 6: Tumor growth in avascular phase.

After necrotic core formation, secreted TAF by hypoxic cells ignites angiogenesis, and accordingly, new growing sprouts provide essential supply such as oxygen to resume tumor accelerating growth [48]. Based on the results from the in-vivo model, in the computational model it is assumed that after 15 days of avascular growing, sprouting angiogenesis begins. Also, considering the experiment set up, at onset of vascular phase, the tumor diameter is around 2 mm. In Fig. 7, initial phase of tumor vascular growth is shown in the three days periods. Fig. 7 illustrates that due to local oxygen concentration increases, proliferating cells accelerate their

growth. However, pay attention that the quiescent region is still developing (Fig. 7). Consequently, the proliferating cells gain the required oxygen supply for unleashed growing, and by these mean, the activated quiescent cells found the opportunity to grow and proliferate due to reducing physical stresses in the surrounding. Fig. 9 shows the computational results on day 15^{th} to day 24^{th} of vascular tumor growth. Results for day 15^{th} and 18^{th} prove that the quiescent cells are activating, and switching to proliferating phenotype. Subsequently, the tumor size increases more than twice in just these three days. Finally, must of the quiescent cells start to grow again which made the tumor growth gradient rises dramatically (Fig. 9).

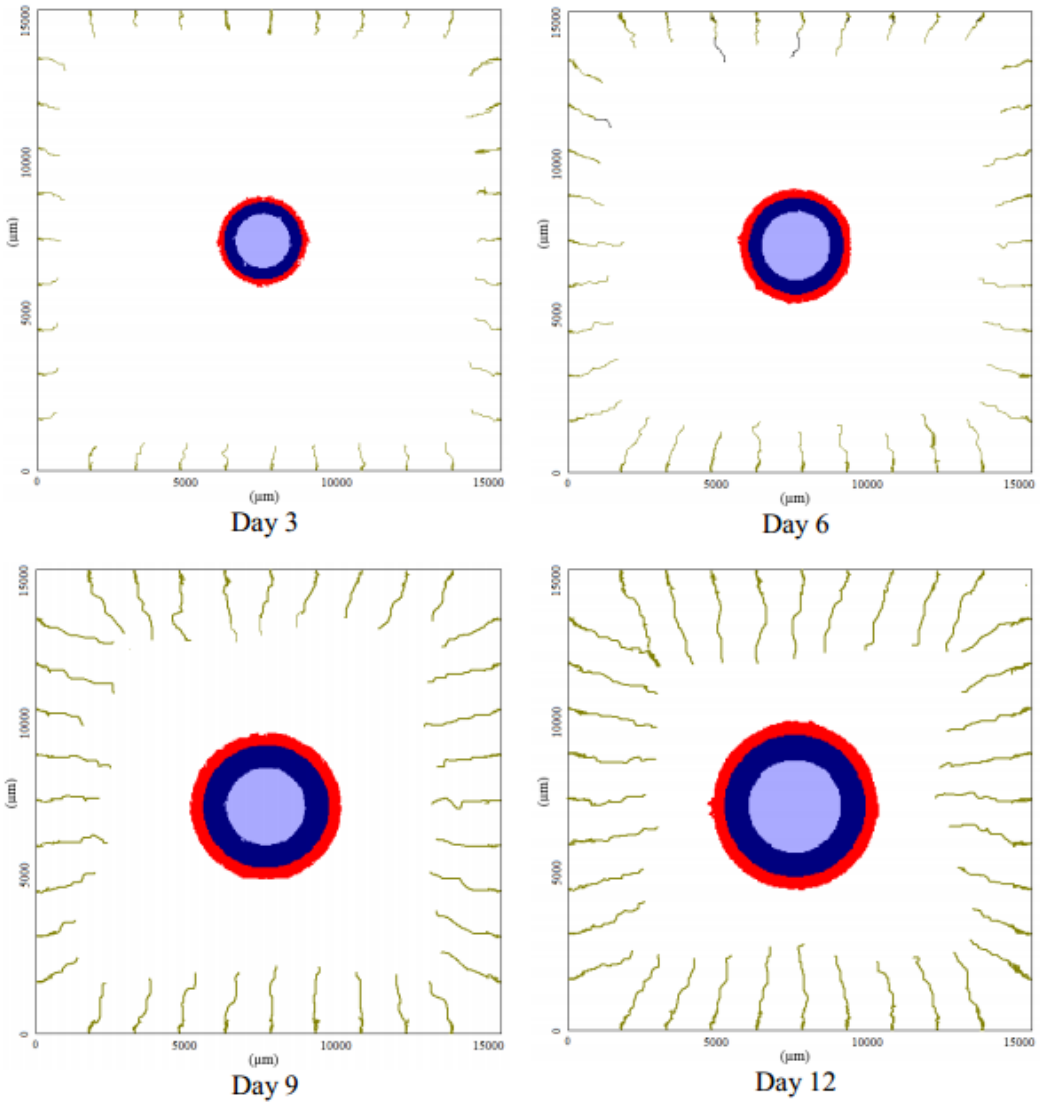

Figure 7: Tumor growth during a 12 days period after initiation of angiogenesis. Sprouts grow toward tumor and also, the oxygen concentration locally rises.

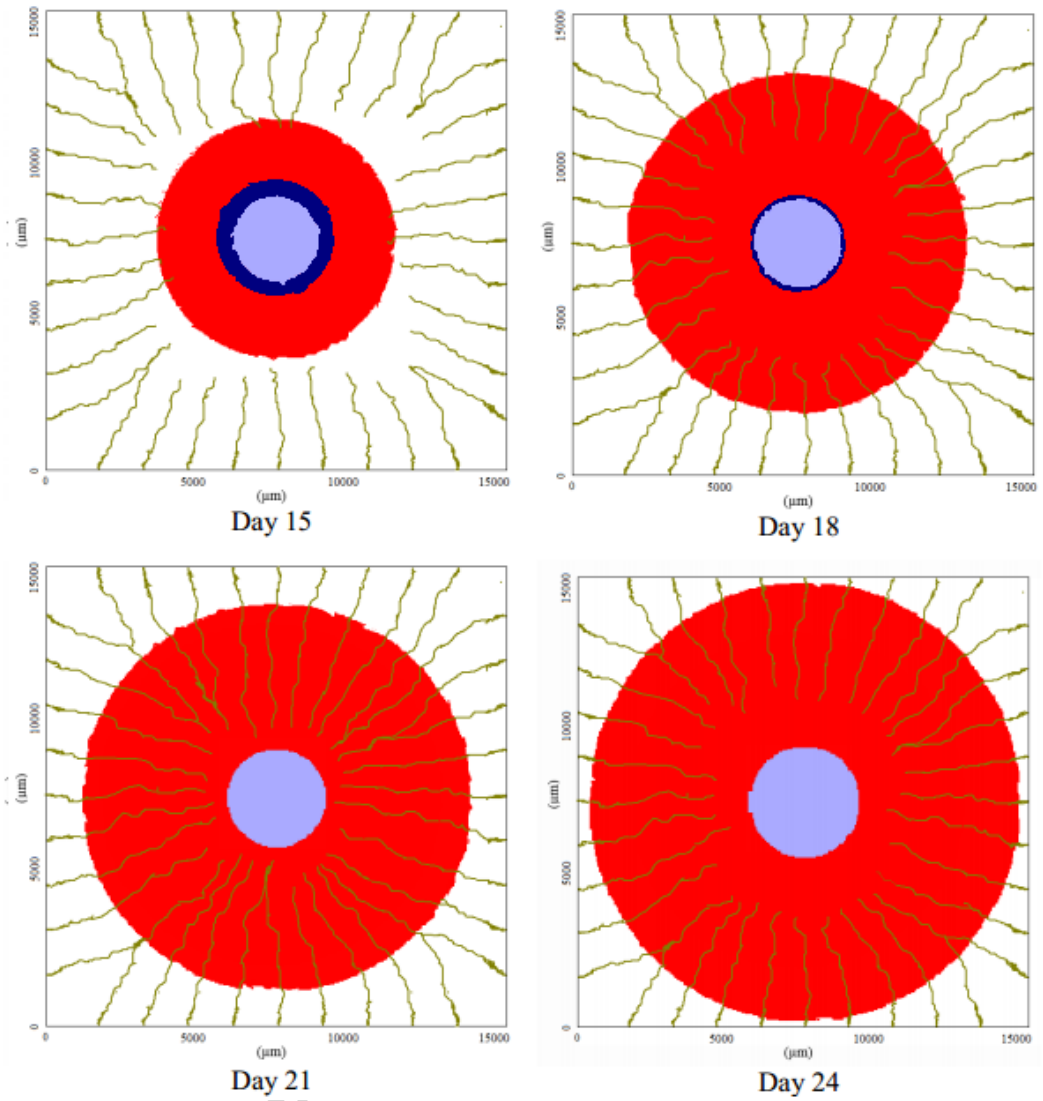

Figure 8: Tumor growth during second 12 days of vascular growth. After tumor vascularization, tumor starts to grow exponentially.

Fig 8 depicts that the anastomosis, which in the connection of at least two sprouts, is happening during angiogenesis. In Fig. 9 the computational results on vascular tumor growth are compared with the one of the experimental observations. Accordingly, Fig 9. Shows that the model successfully is able to reproduce the trend of the solid tumor growth.

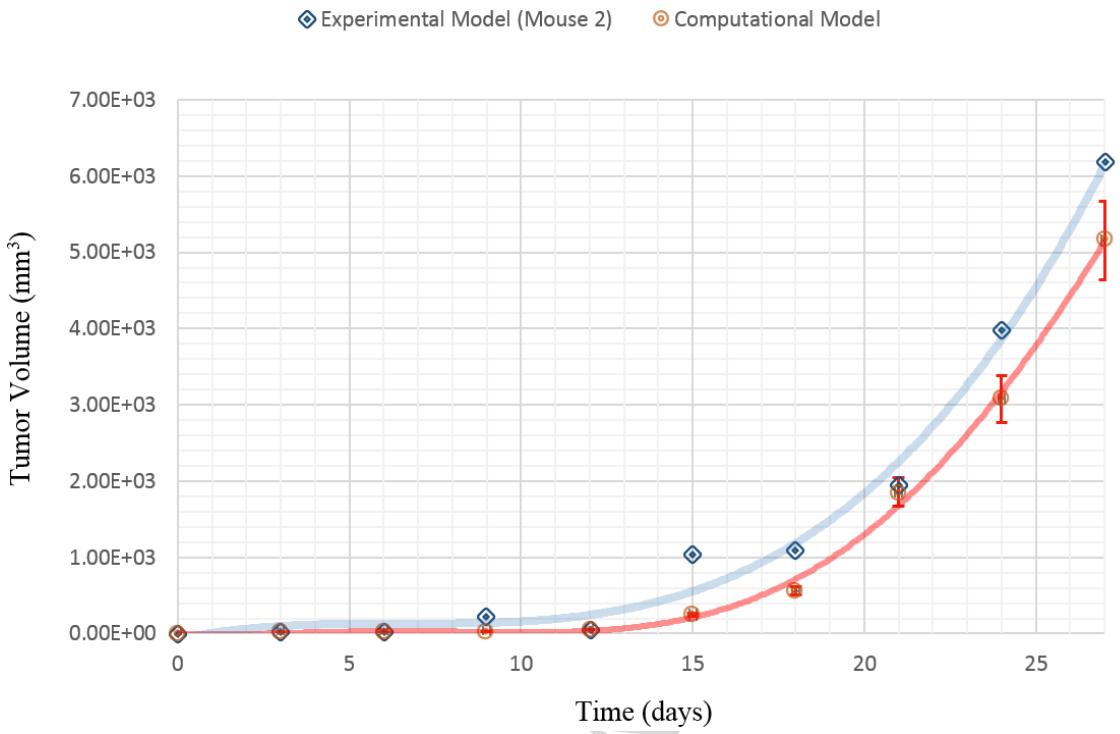

Figure 9: A diagram on tumor vascular growth. Considering the simplifications and assumptions in the computational model, the trend of numerical results (red line) show a good convergence with the experimental results.

Conclusions

Clinical evidences shown that the growth of a tumor is in two different phases. While avascular growth of tumors is likely to be benign, the vascular tumor is malignant and ignites tumor invasion. In this study by using a comprehensive multi-scale model, a realistic model for tumor growth has been developed. Considering the nature of a solid tumor, the cellular environment of tumor was modeled in respect to the various cells phenotype including proliferating, quiescent and necrotic cells. Also, the model successfully simulated the complete process of tumor growth including avascular growth, angiogenesis and vascular growth. Moreover, the model coupled the

three interconnected level including extracellular, cellular and intracellular levels by implementing biologically desired approaches. At the extracellular level, PDEs described the oxygen and TAF diffusion in the domain. At the cellular level, CPM simulated the cellular dynamics in tissue microenvironment. Finally, at the intracellular level, few biophysical and biochemical rules controlled each cell internal machine. The results incorporate that angiogenesis is the main reason toward increasing growth rate at vascular phase. Accordingly, comparing with vascular tumor growth, avascular tumor growth rate is negligible. Furthermore, we evaluated the computational model in vascular stage using an in-vivo model. Although the model consists of a series of simplifications and assumptions, however, the final results shown a good coherence to the experimental observations as well as prior computational models. Also, the simulation was based on a biologically desired modeling, which considering the governing role of microenvironment on cancer dynamics, the current model would enable us to examine the effect of therapeutic mechanisms such as chemotherapy and radiotherapy on the tumor cellular dynamics.

Acknowledgement

We thank Mr. M. Haji Akhoundzadeh for assistance with preparing the manuscript.

References

1. Brown JM, Giaccia AJ. The unique physiology of solid tumors: opportunities (and problems) for cancer therapy. Cancer research. 1998;58(7):1408-16. Epub 1998/04/16. PubMed PMID: 9537241.

2. Araujo RP, McElwain DLS. A history of the study of solid tumour growth: The contribution of mathematical modelling. Bulletin of Mathematical Biology. 2004;66(5):1039. doi: 10.1016/j.bulm.2003.11.002.

3. McMahon G. VEGF receptor signaling in tumor angiogenesis. The oncologist. 2000;5 Suppl 1:3-10. Epub 2000/05/10. PubMed PMID: 10804084.

4. Takaoka A, Adachi M, Okuda H, Sato S, Yawata A, Hinoda Y, et al. Anti-cell death activity promotes pulmonary metastasis of melanoma cells. Oncogene. 1997;14(24):2971-7. Epub 1997/06/19. doi: 10.1038/sj.onc.1201147. PubMed PMID: 9205104.

5. Hanahan D, Folkman J. Patterns and Emerging Mechanisms of the Angiogenic Switch during Tumorigenesis. Cell. 86(3):353-64. doi: 10.1016/S0092-8674(00)80108-7.

6. Mustonen T, Alitalo K. Endothelial receptor tyrosine kinases involved in angiogenesis. The Journal of cell biology. 1995;129(4):895-8. Epub 1995/05/01. PubMed PMID: 7538139; PubMed Central PMCID: PMCPMC2120485.

7. Paweletz N, Knierim M. Tumor-related angiogenesis. Critical reviews in oncology/hematology. 1989;9(3):197-242. Epub 1989/01/01. PubMed PMID: 2480145.

8. Folkman J. Tumor angiogenesis: therapeutic implications. The New England journal of medicine. 1971;285(21):1182-6. Epub 1971/11/18. doi: 10.1056/nejm197111182852108. PubMed PMID: 4938153.

9. Bauer AL, Jackson TL, Jiang Y. A cell-based model exhibiting branching and anastomosis during tumor-induced angiogenesis. Biophysical journal. 2007;92(9):3105-21. Epub 2007/02/06. doi: 10.1529/biophysj.106.101501. PubMed PMID: 17277180; PubMed Central PMCID: PMCPMC1852370.

10. O'Connor JPB, Aboagye EO, Adams JE, Aerts HJWL, Barrington SF, Beer AJ, et al. Imaging biomarker roadmap for cancer studies. Nat Rev Clin Oncol. 2016;advance online publication. doi: 10.1038/nrclinonc.2016.162

11. Copeland TP, Creasman JM, Seidenwurm DJ, Franc BL. Contextualizing the use of oncologic imaging within treatment phases: imaging trends and modality preferences, 2000–2014. Current Oncology. 2017;24(2):e99-e105. doi: 10.3747/co.24.3216. PubMed PMID: PMC5407885.

12. Hogea CS, Murray BT, Sethian JA. Simulating complex tumor dynamics from avascular to vascular growth using a general level-set method. Journal of mathematical biology. 2006;53(1):86-134. Epub 2006/06/23. doi: 10.1007/s00285-006-0378-2. PubMed PMID: 16791651.

13. Mansury Y, Deisboeck TS. Modeling Tumors as Complex Biosystems: An Agent-Based Approach. In: Deisboeck TS, Kresh JY, editors. Complex Systems Science in Biomedicine. Boston, MA: Springer US; 2006. p. 573-602.

14. Mente C, Voss-Böhme A, Deutsch A. Analysis of individual cell trajectories in lattice-gas cellular automaton models for migrating cell populations. Bulletin of mathematical biology. 2015 Apr 1;77(4):660-97.

15. Ermentrout GB, Edelstein-Keshet L. Cellular automata approaches to biological modeling. Journal of theoretical Biology. 1993 Jan 7;160(1):97-133.

16. Oden JT, Hawkins A, Prudhomme S. General diffuse-interface theories and an approach to predictive tumor growth modeling. Mathematical Models and Methods in Applied Sciences. 2010 Mar;20(03):477-517.

17. Farnsworth RH, Lackmann M, Achen MG, Stacker SA. Vascular remodeling in cancer. Oncogene. 2014 Jul 3;33(27):3496-505.

18. Ng CF, Frieboes HB. Model of Vascular Desmoplastic Multispecies Tumor Growth. Journal of Theoretical Biology. 2017 May 18.

19. Jiang Y, Pjesivac-Grbovic J, Cantrell C, Freyer JP. A Multiscale Model for Avascular Tumor Growth. Biophysical journal. 2005;89(6):3884-94. doi: 10.1529/biophysj.105.060640. PubMed PMID: PMC1366955.

20. Alemani D, Pappalardo F, Pennisi M, Motta S, Brusic V. Combining cellular automata and lattice Boltzmann method to model multiscale avascular tumor growth coupled with nutrient diffusion and immune competition. Journal of Immunological Methods. 2012 Feb 28;376(1):55-68.

21. Dormann S, Deutsch A. Modeling of self-organized avascular tumor growth with a hybrid cellular automaton. In silico biology. 2002 Jan 1;2(3):393-406.

22. Ghadiri M, Heidari M, Marashi SA, Mousavi SH. A multiscale agent-based framework integrated with a constraint-based metabolic network model of cancer for simulating avascular tumor growth. Molecular BioSystems. 2017;13(9):1888-97.

23. Roose T, Chapman SJ, Maini PK. Mathematical models of avascular tumor growth. Siam Review. 2007 May 1;49(2):179-208.

24. Cristini V, Lowengrub J. Multiscale modeling of cancer: an integrated experimental and mathematical modeling approach. Cambridge University Press; 2010 Sep 9.

25. Oden JT, Lima EA, Almeida RC, Feng Y, Rylander MN, Fuentes D, Faghihi D, Rahman MM, DeWitt M, Gadde M, Zhou JC. Toward predictive multiscale modeling of vascular tumor growth. Archives of Computational Methods in Engineering. 2016 Dec 1;23(4):735-79.

26. Macklin P, McDougall S, Anderson AR, Chaplain MA, Cristini V, Lowengrub J. Multiscale modelling and nonlinear simulation of vascular tumour growth. Journal of mathematical biology. 2009 Apr 1;58(4):765-98.

27. Shirinifard A, Gens JS, Zaitlen BL, Popławski NJ, Swat M, Glazier JA. 3D multi-cell simulation of tumor growth and angiogenesis. PloS one. 2009 Oct 16;4(10):e7190.

28. Lesart AC, Van Der Sanden B, Hamard L, Estève F, Stéphanou A. On the importance of the submicrovascular network in a computational model of tumour growth. Microvascular Research. 2012 Sep 30;84(2):188-204.

29. Tang L, van de Ven AL, Guo D, Andasari V, Cristini V, Li KC, et al. Computational Modeling of 3D Tumor Growth and Angiogenesis for Chemotherapy Evaluation. PLOS ONE. 2014;9(1):e83962. doi: 10.1371/journal.pone.0083962.

30. Xu J, Vilanova G, Gomez H. A Mathematical Model Coupling Tumor Growth and Angiogenesis. PLOS ONE. 2016;11(2):e0149422. doi: 10.1371/journal.pone.0149422.

31. Graner F, Glazier JA. Simulation of biological cell sorting using a two-dimensional extended Potts model. Physical review letters. 1992 Sep 28;69(13):2013.

32. Voss-Böhme A. Multi-Scale Modeling in Morphogenesis: A Critical Analysis of the Cellular Potts Model. PLOS ONE. 2012;7(9):e42852. doi: 10.1371/journal.pone.0042852.

33. Beysens DA, Forgacs G, Glazier JA. Cell sorting is analogous to phase ordering in fluids. Proceedings of the National Academy of Sciences. 2000 Aug 15; 97(17):9467-71.

34. Varennes J, Han B, Mugler A. Collective chemotaxis through noisy multicellular gradient sensing. Biophysical journal. 2016 Aug 9;111(3):640-9.

35. Maire T, Youk H. Molecular-level tuning of cellular autonomy controls the collective behaviors of cell populations. Cell systems. 2015 Nov 25;1(5):349-60.

36. Sefidgar M, Soltani M, Raahemifar K, Sadeghi M, Bazmara H, Bazargan M, Naeenian MM. Numerical modeling of drug delivery in a dynamic solid tumor microvasculature. Microvascular research. 2015 May 1;99:43-56.

37. Bazmara H, Soltani M, Sefidgar M, Bazargan M, Naeenian MM, Rahmim A. Blood flow and endothelial cell phenotype regulation during sprouting angiogenesis. Medical & biological engineering & computing. 2016 Mar 1;54(2-3):547-58.

38. Mueller-Klieser W, Freyer JP, Sutherland RM. Influence of glucose and oxygen supply conditions on the oxygenation of multicellular spheroids. British journal of cancer. 1986 Mar;53(3):345.

39. Mueller-Klieser W. Method for the determination of oxygen consumption rates and diffusion coefficients in multicellular spheroids. Biophysical journal. 1984 Sep 1;46(3):343-8.

40. Freyer JP. Rates of oxygen consumption for proliferating and quiescent cells isolated from multicellular tumor spheroids. InOxygen Transport to Tissue XV 1994 (pp. 335-342). Springer, Boston, MA

41. Freyer JP, Sutherland RM. Proliferative and clonogenic heterogeneity of cells from EMT6/Ro multicellular spheroids induced by the glucose and oxygen supply. Cancer Research. 1986 Jul 1;46(7):3513-20.

42. Serini G, Ambrosi D, Giraudo E, Gamba A, Preziosi L, Bussolino F. Modeling the early stages of vascular network assembly. The EMBO journal. 2003 Apr 15;22(8):1771-9.

43. Carmeliet P. VEGF as a key mediator of angiogenesis in cancer. Oncology. 2005;69(Suppl. 3): 4-10.

44 Leith JT, Michelson S. Secretion rates and levels of vascular endothelial growth factor in clone A or HCT-8 human colon tumour cells as a function of oxygen concentration. Cell proliferation. 1995 Aug 1;28(8):415-30.

45. Bauer AL, Jackson TL, Jiang Y. Topography of extracellular matrix mediates vascular morphogenesis and migration speeds in angiogenesis. PLoS computational biology. 2009 Jul 24;5(7):e1000445.

46. Bazmara H, Soltani M, Sefidgar M, Bazargan M, Naeenian MM, Rahmim A. The vital role of blood flow-induced proliferation and migration in capillary network formation in a multiscale model of angiogenesis. PloS one. 2015 Jun 5;10(6):e0128878.

47. Salavati H, Soltani M, Bazmara H. Investigation on the effect of inosculation strategy on promoting vascularization in tissue engineering. Modares Mechanical Engineering. 2016; 16(4): 29-40 (In Persian).

48. Soltani M. Numerical modeling of drug delivery to solid tumor microvasculature. Waterloo, Ontario, Canada, PhD thesis in Chemical Engineering. 2013 Jan.

"Highlights"

- Modeling the major phases involved in tumor growth including avascular and vascular growth as well as angiogenesis.

- The modeling strategy is multi-scale, and it covers extracellular, intercellular and intracellular dynamics.

- An animal study confirms the ability of the model to simulate solid tumor growth.

- As the simulation and in-vivo experiment shows, the progression of tumor is highly depends on the angiogenesis process.